Macromolecules
ARTICLE

Macromolecules **2010**, *43*, 8275–8281 **8275**
DOI: 10.1021/ma101240j

Segmental Dynamics in PMMA-Grafted Nanoparticle Composites

Pinar Akcora* and Sanat K. Kumar*

Department of Chemical Engineering, Columbia University, New York, New York 10027

Victoria García Sakai

NIST Center for Neutron Research, National Institute of Standards and Technology, Gaithersburg, Maryland 20899

Yu Li and Brian C. Benicewicz

Department of Chemistry and Biochemistry, University of South Carolina, Columbia, South Carolina 29208

Linda S. Schadler

Department of Materials Science and Engineering, Rensselaer Polytechnic Institute, Troy, New York 12180

Received June 4, 2010; Revised Manuscript Received July 22, 2010

ABSTRACT: We have recently shown that silica nanoparticles grafted with polystyrene chains behave akin to block copolymers due to the "dislike" between the nanoparticles and the grafts. These decorated nanoparticles, thus, self-assemble into various morphologies, from well-dispersed nanoparticles to anisotropic superstructures, when they are placed in homopolystyrene matrices of different molecular masses. Here, we consider a slightly different case, where the grafted chains and the matrix (both PMMA) are strongly attracted to the silica nanoparticle surface. We then conjecture that these systems show phase mixing or demixing depending on the miscibility between the brush and matrix chains ("autophobic dewetting"). At 15 mass % particle loading, composites created using the same grafted nanoparticle, but with two different matrices, yield well dispersed nanoparticles or nanoparticle "agglomerates", respectively. Rheology experiments show that the composites display solid-like behavior only when the particles are aggregated. As deduced in previous work, this difference in behavior is attributed to the presence of percolating particle clusters in the agglomerated samples which allows for stress propagation through the system. Going further, we compare the local mobility of matrix and grafted segments of both composites using quasi-elastic neutron scattering experiments. For the liquid-like system, the mean square displacements of the grafted chains and matrix chains, the particle structuring and mechanical response are all unaffected by annealing time. In contrast, in the reinforced case, only the local matrix motion is unaffected by time. Since the particle clustering and solid-like mechanical reinforcement increase with increasing time, we conclude that mechanical reinforcement in polymer nanocomposites is purely based on the nanoparticles, with essentially no "interference" from the matrix. In conjunction with other results in the literature, we then surmise that mechanical reinforcement is caused by the bridging of particles by the grafted polymer layers and not due to the formation of "glassy" polymer layers on the nanoparticles.

I. Introduction

Polymer−particle interactions play an important role in controlling the mechanical properties of polymer nanocomposites. There are three distinct scenarios which have been proposed to explain this reinforcement.[1−3] At one extreme, the finite element calculations of Gusev and his co-workers[4] have suggested that mechanical reinforcement occurs due to the agglomeration of particles; if these agglomerates percolate through the system, then, there is a direct pathway for the propagation of stress resulting in mechanical reinforcement. In contrast to this "particle-only" scenario, there are two other proposals where both the particles and polymer chains are involved in mechanical reinforcement. Long and his co-workers[5] used the well accepted fact that chain immobilization occurs around nanoparticles[6]—when these composite particles (i.e., the particles with the "bound" glassy layer) overlap and the resulting structures percolate, then mechanical reinforcement occurs. Evidence for this scenario was deduced by measuring changes in the glass transition temperature on adding nanoparticles to polymers.[7−10] In these situations the "bound" layers are thought to not relax in the experiments because they are glassy, thus leading to reinforcement. A final scenario proposed by Goritz in the context of the Payne effect,[11] and elaborated upon by Wang[12] and Sternstein,[13] is that the particles form a network, with the polymer chains forming the "bridges" between the particles. There are several experiments which have been proposed to support each of these different scenarios, but a comprehensive understanding is still elusive. In the work presented here, we attempt to resolve between these different scenarios, especially the polymer−particle based ones, by simultaneously measuring the macroscale mechanical reinforcement and local segmental dynamics in two nanocomposites, one which shows strong mechanical reinforcement while the

*Corresponding author.

Published on Web 09/10/2010

Table 1. PMMA Composites Used in the QENS Experiments[a]

	matrix chains (polymer)	tethered chains (on SiO_2 particles)	grafting density (chains/nm^2)
composite A (immiscible)	d-PMMA[b,c] M_w = 188.6 kg/mol PDI: 1.04	h-PMMA-gr-Si[e] M_w = 55 kg/mol PDI: 1.38	0.12
composite B (miscible)	d-PMMA[b,c] M_w = 18 kg/mol PDI: 1.15	h-PMMA-gr-Si[e] M_w = 55 kg/mol PDI: 1.38	0.12
composite C (immiscible)	h-PMMA[c,d] M_w = 207.4 kg/mol PDI: 1.02	d-PMMA-gr-Si[f] M_w = 60 kg/mol PDI: 1.20	0.05
composite D (miscible)	h-PMMA[c,d] M_w = 10.2 kg/mol PDI: 1.03	d-PMMA-gr-Si[f] M_w = 60 kg/mol PDI: 1.20	0.05

[a] The silica amount is 15 mass % in all composites. [b] deuterated PMMA (d-PMMA). [c] purchased from Polymer Laboratories. [d] hydrogenated PMMA (h-PMMA). [e] hydrogenated PMMA grafted on silica nanoparticles. [f] deuterated PMMA grafted on silica nanoparticles.

other one does not. Since the two composites also have different spatial distributions of the particles, we can then deduce the molecular bases for reinforcement in this class of materials.

Confinement Effects on Chain Dynamics. The effect of chain "confinement" on local dynamics has been observed at the interfaces of thin films[14,15] and in bound polymer layers around nanoparticles formed due to the attraction between the polymer and the nanoparticles.[2,16−18] For example, previous work on various polymers (PS, PMMA, TMPC) containing C60 nanoparticles[19] suggests that local segmental motions are suppressed due to the presence of nanoparticles. Quasi-elastic neutron scattering (QENS) has been also used to investigate chain dynamics when PMPS is mixed with silicate sheets. In this specific case, confinement induces an increased mobility of chains in the vicinity of particle surfaces.[16] This behavior has been attributed to the intimate mixing of PMPS chains with the surfactant on the silica sheets−chain motion is then coupled to the relatively mobile surfactants in these confined spaces. Thus, while there has been considerable interest in probing the local motion of polymers in the presence of surfaces, universal behavior is not observed. Instead, the chemical specificity of the situations dictate the behavior observed.

Controlling the Spatial Distribution of Nanoparticles. A central ability that underpins the work presented here is the fact that, in recent experiments, we showed that spherical silica nanoparticles isotropically grafted with polystyrene chains self-assemble into a range of superstructures when they are dispersed into the corresponding homopolymer.[20] The particular structure formed is sensitively determined by grafting density and the ratio of the brush to matrix molecular weights. Theory and simulation show that this assembly is driven by the microphase separation arising from the immiscibility between the inorganic particle core and the polymeric grafted chains—a process analogous to the self-assembly of block copolymer or other amphiphiles. Thus, the use of decorated nanoparticles appears to be a facile means of controlling the spatial distribution of nanoparticles.

Goals of this Paper. Here, we use grafted nanoparticles to study both the macroscale rheology and the segmental dynamics of PMMA based composites where the aggregation state of particles can be systematically varied. The two systems chosen for this study represent extreme cases of particle dispersion: well-dispersed nanoparticles vs anisotropic (apparently percolating) nanoparticle clusters. While the former case shows liquid-like mechanical behavior, the latter displays strong mechanical reinforcement, as characterized by a low frequency plateau in the frequency dependent mechanical storage modulus. The mean-square displacements of protons in these two nanocomposites, probed using elastic scans in quasi-elastic neutron scattering (QENS) experiments show very different temporal behavior. (Note that both the brush chains and the matrix are examined using selective, isotopic labeling.) The matrix polymers' behavior is independent of annealing time in both cases, as are the grafted chain dynamics in the well dispersed case. In contrast, the grafted chain dynamics slow as the particles aggregate in the composite where the particles form anisotropic structures. These data, in combination, clearly show that the mechanical reinforcement is driven purely by the grafted nanoparticles without "interference" from the matrix. Further, based on TEM micrographs, we conjecture that the mechanical reinforcement can be attributed to the formation of a particle network, with the grafted chains providing the mechanical "bridges" between the nanoparticles, rather than due to the overlap of glassy polymer shells around particles.

Table 2. Glass-Transition Temperatures (T_g) Determined from DSC Scans for the Composites and Their Corresponding Homopolymers, Annealed at 145 °C for 2 d and 30 d

sample	T_g (°C) after 2 d annealing	T_g (°C) after 30 d annealing
18 kg/mol PMMA homo	127	128
composite B	126	126
188.6 kg/mol PMMA homo	128	131
composite A	128	132

II. Experimental Section

Nominally spherical silica particles with a diameter of 14 ± 4 nm were obtained from Nissan Chemicals. We used radical addition−fragmentation chain transfer (RAFT) polymerization to "grow" the PMMA chains from the particle surfaces.[21,22] The PMMA-grafted particles were mixed with the homopolymers in toluene, cast onto aluminum cups creating films of approximately 60 μm thickness, and then annealed for various times at 145 °C in vacuum. The samples were characterized by transmission electron microscopy (TEM), differential scanning calorimetry (DSC), quasi-elastic neutron scattering (QENS), and rheology. Since QENS is primarily sensitive to the dynamics of the protons, the segmental dynamics of the graft and the matrix segments can be probed through the use of selective labeling. Four sets of PMMA composite samples were thus examined: hydrogenated PMMA grafted silica particles in matrices of deuterated PMMA of two different masses (M_w = 18 kg/mol and 188.6 kg/mol) and deuterated PMMA grafted particles in protonated PMMA matrices with molecular masses of 207.4 kg/mol and 10.2 kg/mol. Table 1 shows the characteristics of the particles and matrix polymers studied. Note that, while the graft densities for the protonated vs deuterated grafted particles are different, the morphologies which result are not affected by this change. Thus, we compare them on an equal footing, but with the caveat that quantitative comparisons might be difficult.

The glass-transition temperatures of these samples were measured with a TA Instruments' Q100 differential scanning calorimeter (DSC) after 2d and 30d annealing, respectively. Table 2 shows the T_g of the composites and their corresponding homopolymers. It is evident that the T_g's of the composite and homopolymer are the same for different annealing times. Any discrepancy in T_g of the composite A annealed for 2d vs 30d thus does not seem to be the result of the particles, since a similar T_g increase is observed in the corresponding homopolymer. The samples were also analyzed after 30 d annealing time using Fourier transform infrared spectroscopy (FT-IR) to verify that

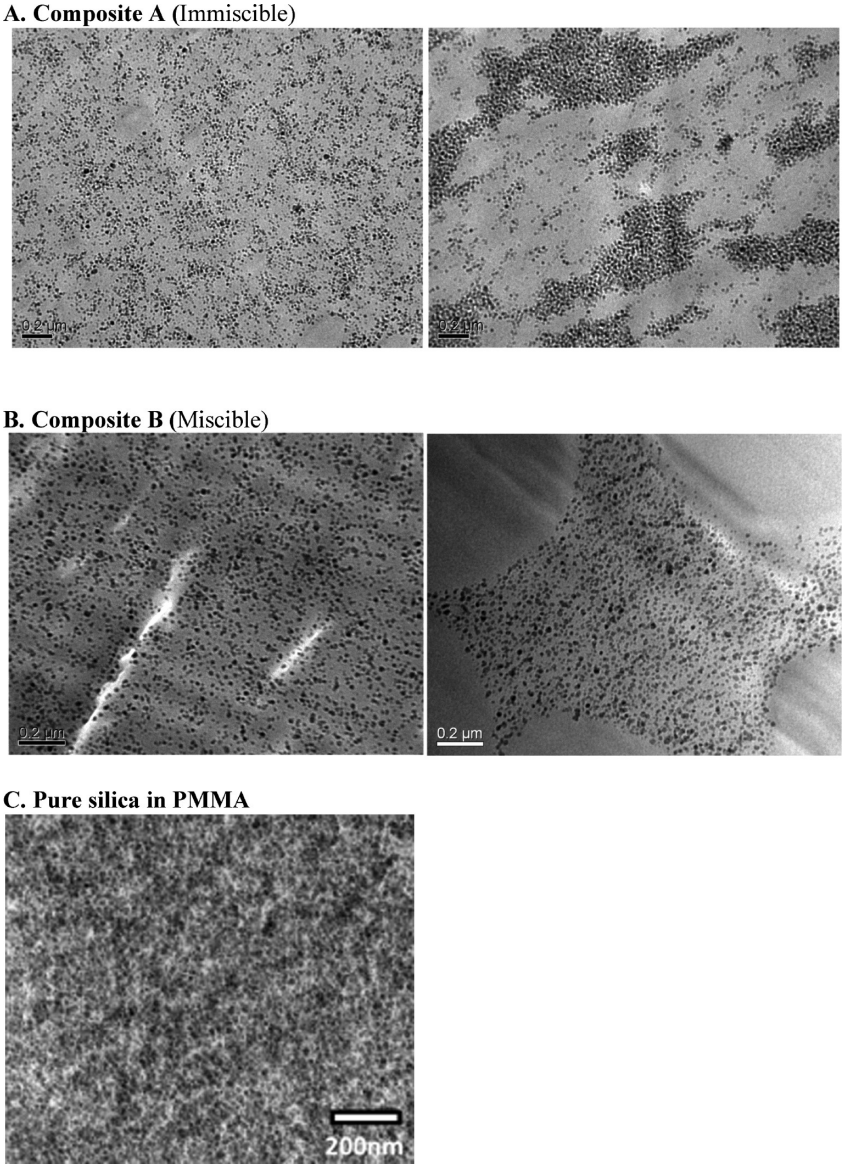

Figure 1. Transmission electron micrographs show the dispersion of PMMA grafted particles in immiscible composite A (part A) and in miscible composite B (part B). Images on the left were taken after 2 d of annealing and on the right after 30 d of annealing. Particle loading is 15 mass % in all samples. Scale bars are 0.2 μm. For reference, we also show the dispersion of bare silica particles in PMMA (100 kg/mol) at 15 mass % loading. Clearly, good dispersion is seen in this last case, where the samples were annealed for 5 days.

there was no degradation during the long annealing process or during the scattering measurements, performed well above the T_g of the composites.

Samples for electron microscopy (Jeol JEM-100 CX) analysis were prepared by ultramicrotomy. Samples for rheology were solution cast in air and annealed for 2 d and 30 d at 150 °C. Dynamic oscillatory experiments were then performed in a TA Instruments' AR2000 rheometer using the 8 mm parallel plates under nitrogen.

The QENS measurements were performed on the NG2 high-flux backscattering spectrometer at the NIST Center for Neutron Research in Gaithersburg, MD.[23] The neutrons are Doppler shifted about an incident wavelength of 6.27 Å to provide a range of incoming neutron wavelengths while the final energy is fixed by scattering from crystal analyzers to the detectors. With the Doppler stationary, elastic window scans were performed while heating the samples from 50 to 500 K at a heating rate of 1 K/min.

SAXS measurements were performed on beamline X27C at the Brookhaven National Laboratories using 9 keV electrons at room temperature. The data were analyzed by fitting it to the Beaucage unified model equation:[24,25]

$$I(q) = \sum_i A_i \exp[-q^2 {R_{gi}}^2/3] + B_i \left[\frac{\mathrm{erf}\left(\frac{qR_{gi}}{\sqrt{6}}\right)^3}{q}\right]^{p_i}$$

where q is the scattering vector, R_g is the particle size, A is the exponential prefactor, B is the Porod constant, and p is the power law exponent. We assume that particle structures are hierarchical, and the structure at hierarchy i have radius of gyration, R_{gi}.[24,26] In our previous work on similar nanocomposites,[20] we had compared the parameters obtained from SAXS data fits with TEM micrographs and shown that these two descriptions yield similar information on particle structuring. Here, we further note that it is not easy to directly interpret these scattering patterns without fits because the SAXS does not go to low enough q values to pick-up all levels

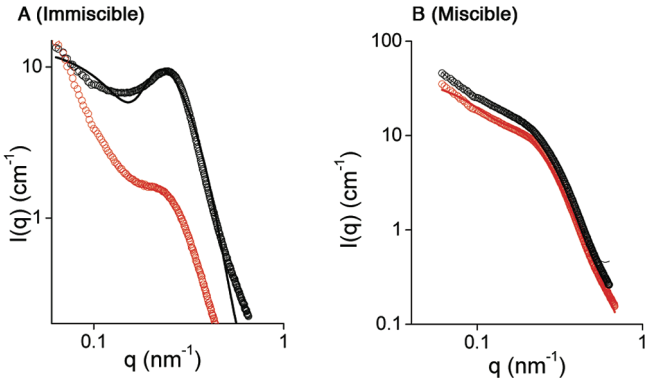

Figure 2. SAXS data for PMMA-grafted silica (31 kg/mol) in 207 kg/mol (A, immiscible) and 52 kg/mol (B, miscible) PMMA matrices for different annealing times (1 and 7 d at 145 °C). Red symbols are for the 1 d and black symbols are for the 7 d annealed composites. Grafting density is 0.12 chains/nm^2 and particle loading is 5%. The lines are the unified fits. Fit parameters are shown in Table 3.

of structure, especially when the particles agglomerate into percolated structures.

III. Results and Discussion

Morphology. PMMA composites containing 15 mass % particles were prepared and annealed for 2d and 30d, respectively. Transmission electron micrographs of Composites A and B (Table 1) show particle morphologies as a function of annealing time (Figure 1). SAXS measurements were used to verify these conclusions, as in our past work.[20] In the case of the low molecular weight matrix (sample B) we see that the particles are well dispersed. This miscible composite shows essentially no significant change in particle dispersion with annealing (Figure 1B), as confirmed by SAXS results (Figure 2B). The primary particle size (R_g) obtained from the fit was ~10 nm, which did not change in the annealed composite. The unified fit parameters are given in Table 3. While the samples run in SAXS are not identical to the samples characterized in the rest of the paper, the ratio of brush and matrix chain lengths representing the miscible and immiscible composites are close (see the composite characteristics in Figure 2). The particles dispersed in the high molecular weight matrix (sample A) aggregate into micrometer-size clusters. The aggregation state presumably increases with annealing time as stronger interference between scatterers is observed with a stronger peak in SAXS data (Figure 2A). The structure factor for hard spheres, described by the Percus−Yevick model,[27,28] is included in the unified fits. The particle volume fraction is 0.15 and the mean radius is obtained as 25 nm (parameters for the P−Y prediction are in Table 3). Miscible composites give surface fractal structures with power law exponent of 2. The fractal dimension increases from 2 to 3 when scattering arises from larger scale structures.[29]

This behavior appears to closely track that seen for polystyrene grafted silica particles placed in a polystyrene homopolymer matrix. In that case, good particle dispersion was obtained when the matrix was much smaller in molecular weight than the brush, while superstructure formation reminiscent of Figure 1A was found when the matrix molecular weight becomes large. However, we note one salient point: the polystyrene grafted silica nanoparticles form structures driven by the dislike between the hydrophilic silica core and the hydrophobic polymer graft (or shell). The grafted PMMA would not have been expected to behave in an analogous manner since the silica and PMMA interact strongly through

Table 3. Unified Fit Parameters for SAXS Data

sample	primary particle size (nm)	low-q power law exponent	parameters for Percus−Yevick prediction
31K brush in 52K matrix (1 d), Figure 2B	10	2	
31K brush in 52K matrix (7 d), Figure 2B	10	2	
31K brush in 207K matrix (1 d), Figure 2A, red symbols	15	3	
31K brush in 207K matrix (7 d), Figure 2A, black symbols	15	3	particle size:, 15 nm; mean radius, 25 nm; volume fraction, 0.15

hydrogen bonding interactions. Evidence for this fact is seen in Figure 2C where we show that bare silica particles are well dispersed in PMMA. Thus, the interaction between the nanoparticle and the grafted chains should be attractive, and hence the grafted particle should not behave akin to a surfactant. In this context we note the previous work of Wang and his co-workers,[30] who used polystyrene cores grafted with polybutadiene. When placed in a polybutadiene matrix, whose length is longer than the brush, they found that the particles phase separated from the matrix. While the structures formed by these particles were initially nonspherical, eventually (after several years of annealing) they "equilibrated" into spherical domains. Presumably, the nonspherical morphologies are caused by the phase separation between the brushes and matrix, with the domains becoming spherical at long enough times. This conjecture, which is based on the assumption that the particle core is a passive player in this case, would rationalize our findings on the PMMA grafted particles in the context of our own expectations and intuition.

Macroscale Dynamics and Rheology. Composites A and B (Table 1) have been used for rheology and for characterizing T_g's using differential scanning calorimetry. There was only a 4 °C increase in the T_g of immiscible blend (composite A) after annealing, and no change in T_g was observed for the miscible case (composite B) (Table 2). Thus, the T_g measurements do not yield any significant insights into the macroscale dynamics of these nanocomposites.

In contrast, (linear) oscillatory shear experiments gave very different results in the two cases. The miscible composite (Figure 3) shows no hint of elastic (or solid-like) mechanical response at the highest particle loading tested. This sample consists of matrix PMMA homopolymer with 18 kg/mol, which is higher than the entanglement molecular weight of PMMA (10 kg/mol). Further, since the rheology data were independent of annealing time, we conclude that this sample, which is presumably at equilibrium, does not show mechanical reinforcement. The behavior of the immiscible composite with 15 mass % particles is very different (Figure 3). Samples annealed for 2 and 30 d showed elastic behavior in that the elastic (storage) modulus displayed a low-frequency plateau in both cases. Since this plateau modulus increased by nearly an order of magnitude on annealing, we conclude that the temporal changes in particle dispersion cause this sample to become more solid-like in its mechanical response. Note that the particle agglomeration increased (dramatically) with annealing time, implying the importance of this quantity on mechanical behavior (Figure 1). We explore this issue in more detail below.

There is a question as to whether these differences in behavior may simply be attributed to the different matrix molecular weights employed, especially the low matrix molecular mass in the case where we see no reinforcement. Here,

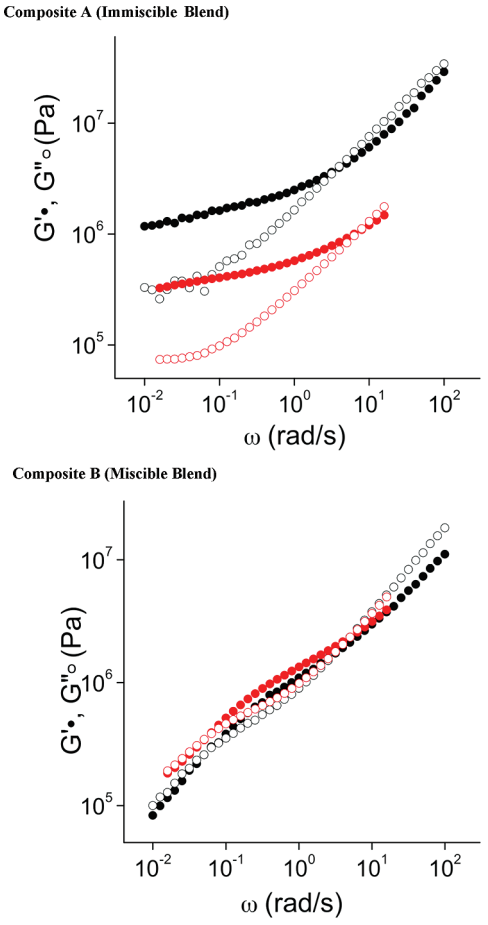

Figure 3. Linear rheology measurements for immiscible (composite A) and miscible (composite B) composites at 160 °C with 5% strain amplitude. Red symbols are for 2 d and black symbols are for 30 d annealed samples. Particle loading is 15 mass % in both composites. Filled symbols correspond to G', open symbols to G''.

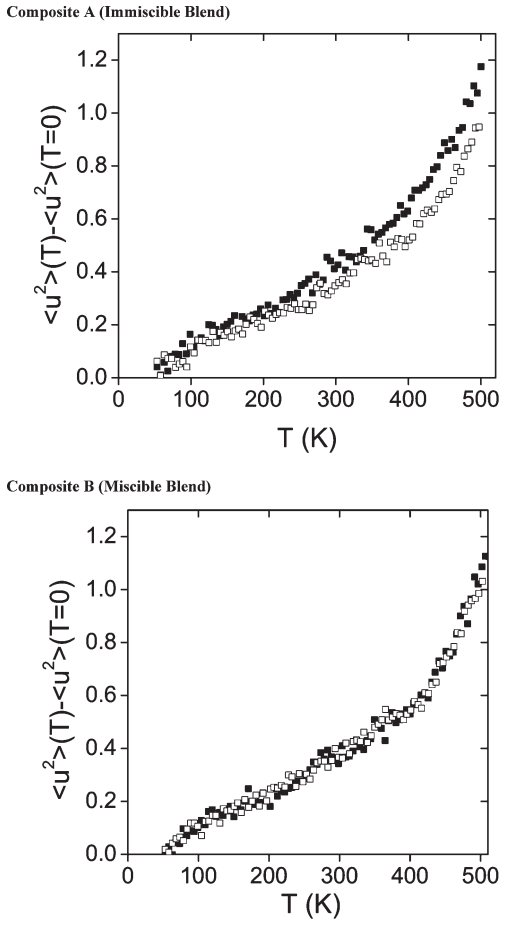

Figure 4. Mean-square displacements of grafted segments of 2 d (filled symbol) and 30 d (open symbol) annealed composites. Particle loading is 15 mass %.

we point to our previous work on PS based composites,[31] where we showed that the matrix molecular weight is not the cause of the differences in behavior seen for the composites. As another supporting piece of evidence we have compared the relaxation times of miscible and immiscible composites in their annealed state, which are calculated from the crossover of G' and G'' using the relationship, $\tau = G'/\omega G''$. The crossover in both sets of data appear around 0.25 s, which shows that the relaxation time in both composites are comparable and not affected by the entanglement of the matrix. Also, the magnitude of loss and storage moduli is comparable in miscible and immiscible composites. On the basis of all these facts, we conclude that entanglement of the matrix polymer does not influence the storage modulus and the solid-like behavior of composites.

QENS Results. In a fixed window neutron scan, the elastic scattering intensity is typically measured as a function of temperature. This intensity drops with increasing temperature as the dynamics of the molecules becomes more pronounced, thus increasing any inelastic scattering contributions. In the Gaussian approximation, the elastic intensity can be quantified by a Debye−Waller factor (DWF) as

$$I_{elastic} = I_0 \exp\left\{-\left(\frac{Q^2}{3}\right)\langle u^2\rangle\right\}$$

where $\langle u^2\rangle$ is the mean-square displacement of the scattering centers calculated for Q values between 0.62 and 1.68 Å^{-1} in our measurements. Note that the incoherent scattering cross-section of the hydrogen atoms is 40 times larger than that from deuterium atoms. In composites C and D, the incoherent scattering from the protonated matrix will dominate the overall signal. At a loading of 15 weight % of the particle cores, the brush constitutes 25% by weight of the sample, while the matrix constitutes the remaining 60%. The amount of matrix and brush are roughly different by a factor of 2. Thus, in all of our samples, the QENS are primarily sensitive to the protonated component in the system, and selective deuteration allows us to separately delineate the dynamics of the matrix and grafted chains.

The elastic scattering measurements show that the mean-square displacements of the grafted chains slightly decreases as the particles agglomerate with annealing (Figure 4, composite A). Apparently, the initial nonequilibrium state has a larger local "free volume": this obviously decreases as the particles aggregate into nonspherical clusters, where they are more proximate, and the system evolves temporally. On the other hand, the mobility of the grafted chains in the miscible blend is practically unchanged on annealing (Figure 4, composite B). This is consistent with TEM results, which show no change in particle dispersion with annealing in Figure 1.

The $\langle u^2\rangle$ values of the matrix chains did not change upon annealing of the two composites C and D (Figure 5). The slower segmental motions of matrix polymer in miscible composite D compared to that of the pure homopolymer (10.2 kg/mol) is probably due to the penetration of matrix chains into grafted domains.

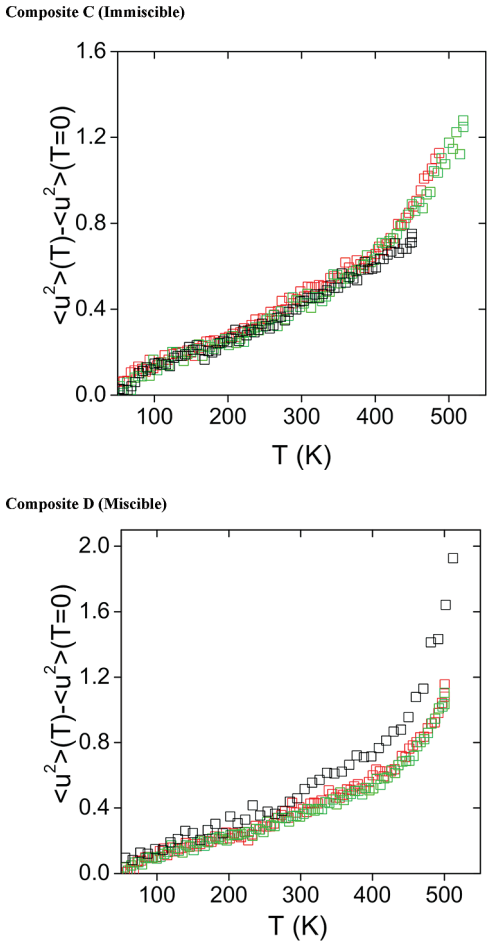

Figure 5. Mean-square displacements of matrix segments in 2 d (red) and 30 d (green) annealed composites. Molecular mass of matrix PMMA homopolymers (black symbols) are 207.4 kg/mol in composite C and 10.2 kg/mol in composite D.

Discussion. *Mechanism of Mechanical Reinforcement.* Our results allow us to conjecture on the mechanism of mechanical reinforcement in these grafted particle based nanocomposites. First, it is apparent that the matrix dynamics are apparently unaffected by the state of particle dispersion, and the mechanical properties which result. To zeroth order, we conclude that the mechanical behavior of such nanocomposites are not related to the matrix, but rather to the particles. Obviously, the particles must percolate through the system for solid-like mechanical behavior to be observed.

Looking in more detail, the outstanding question is if mechanical reinforcement can be attributed to the formation of a glassy polymer layer around the particles (as proposed by Long and co-workers[32−37]) or due to the formation of polymer bridges between the nanoparticles. To resolve this issue we use several pieces of indirect evidence. Previous work on several polymers near silica nanoparticles suggest that there is a bound layer formed on the particles. While some previous estimates had suggested that the bound layer thickness is temperature dependent and as large as 10 nm[33]—the emerging evidence in the past few years, suggest it to be much smaller (∼ 1 nm in thickness) and apparently temperature independent.[8,18,38] Since the interparticle, face-to-face spacings even in the agglomerated state (∼10 nm) are much larger than this quantity, it is immediately apparent that the overlap of glassy layers cannot be responsible for the experimental mechanical results reported here. Second, it is important to note that rheology experiments were conducted at a temperature of 160 °C, well above the glass transition temperature of the polymers in question. At these temperatures it is unclear if the bound layers are glassy. On the basis of these arguments, we conjecture that mechanical reinforcement in these situations is driven by the formation of a particle network with the grafted polymers providing the interparticle bridges. This picture strongly supports the earlier arguments of Sternstein[13,39,40] and of Wang[12] and provides a systematic means of understanding how the addition of nanoparticles affects the mechanical properties of the polymers.

Differences of This System from Previous Results on PS-Based Composites. Our previous work showed that well dispersed nanoparticles with PS grafts displayed solid-like behavior at a loading of 15 weight % silica. In contrast, PMMA-grafted particles which are uniformly distributed show liquid-like behavior at the same loading. We believe that the differences in behavior arise from the differences in molecular weight of the grafted chains in the two cases. In the PS case, the brush molecular weight was ∼100 kg/mol, while the PMMA brushes are only ∼55 kg/mol. Thus, the effective size of the particles is smaller for the PMMA grafted case. While we expect that these particles will show solid-like behavior at higher loadings, we have not tested this prediction to date.

Effect of Variation in Graft Density. While rheology, SAXS, TEM characterizations, and QENS experiments to determine graft mobility are performed on composites with the same grafting density (0.12 chains/nm^2), the samples used in the elastic scattering experiments to measure matrix mobility have grafting density of 0.05 chains/nm^2 (composites C and D in Table 1). We note that good dispersion and anisotropic aggregation are obtained at both graft densities when the matrix is small and large, respectively. We therefore surmise that the results reported are not strongly influenced by the differences in graft density, although we suspect that substantial quantitative differences persist making it hard to draw any quantitative conclusions from this analysis.

IV. Conclusions

We conclusively show that the phase separation of polymer grafted nanoparticles from matrix homopolymers is an apparently "universal" property of grafted particle systems. Composites with well-dispersed particles at a particle loading of 15 weight % behave like a liquid, while agglomerated particles yield solid-like behavior. Macroscopic aggregation, achieved by annealing, leads to a larger elastic modulus compared to its unannealed state where the aggregates are smaller. Elastic scattering results indicate that macroscopic phase separation does not influence the local matrix chain dynamics. The segmental mobility of grafted chains slightly decreases with the aggregation of particles. In combination, these results suggest that the mechanical reinforcement in these situations is driven by the formation of a particle network with the grafted polymers providing the bridges. This picture strongly supports the earlier arguments of Sternstein[13,39,40] and of Wang,[12] and provides a systematic means of understanding how the addition of nanoparticles affects the mechanical properties of the polymers.

Acknowledgment. Partial funding for this research was provided by the National Science Foundation Division of Materials Research (S.K.K., P.A., NSF DMR-0804647), and through the Nanoscale Science and Engineering Initiative of the National Science Foundation under NSF DMR-0642573 at RPI (S.K.K., Y.L., L.S.S., B.C.B.). This work utilized facilities supported in

part by the National Science Foundation under Agreement No. DMR-0454672. We acknowledge the support of the National Institute of Standards and Technology, U.S. Department of Commerce, in providing the neutron research facilities used in this work.

References and Notes

(1) Jancar, J. *J. Mater. Sci.* **2008**, *43* (20), 6747–6757.
(2) Bansal, A.; Yang, H.; Li, C.; Cho, K.; Benicewicz, B. C.; Kumar, S. K.; Schadler, L. S. *Nat. Mater.* **2005**, *4* (9), 693–698.
(3) Alcoutlabi, M.; McKenna, G. B. *J. Phys.: Condens. Matter* **2005**, *17* (15), R461–R524.
(4) Gusev, A. A. *Macromolecules* **2006**, *39* (18), 5960–5962.
(5) Long, D.; Sotta, P. *Rheol. Acta* **2007**, *46* (8), 1029–1044.
(6) Vondracek, P.; Schatz, M. *J. Appl. Polym. Sci.* **1977**, *21* (12), 3211–3222.
(7) Tsagaropoulos, G.; Eisenberg, A. *Macromolecules* **1995**, *28* (18), 6067–6077.
(8) Bogoslovov, R. B.; Roland, C. M.; Ellis, A. R.; Randall, A. M.; Robertson, C. G. *Macromolecules* **2008**, *41* (4), 1289–1296.
(9) Sakai, V. G.; Arbe, A. *Curr. Opin. Colloid Interface Sci.* **2009**, *14* (6), 381–390.
(10) Gagliardi, S.; Arrighi, V.; Ferguson, R.; Telling, M. T. F. *Phys. B: Condens. Matter* **2001**, *301* (1−2), 110–114.
(11) Maier, P. G.; GoÃàritz, D. *KGK-Kautsch. Gummi Kunstst.* **1996**, *49* (1), 18–21.
(12) Zhu, Z.; Thompson, T.; Wang, S. Q.; Von Meerwall, E. D.; Halasa, A. *Macromolecules* **2005**, *38* (21), 8816–8824.
(13) Zhu, A. J.; Sternstein, S. S. *Compos. Sci. Technol.* **2003**, *63* (8), 1113–1126.
(14) Jones, R. L.; Kumar, S. K.; Ho, D. L.; Briber, R. M.; Russell, T. P. *Nature* **1999**, *400* (6740), 146–149.
(15) Shin, K.; Obukhov, S.; Chen, J. T.; Huh, J.; Hwang, Y.; Mok, S.; Dobriyal, P.; Thiyagarajan, P.; Russell, T. P. *Nat. Mater.* **2007**, *6* (12), 961–965.
(16) Chrissopoulou, K.; Anastasiadis, S. H.; Giannelis, E. P.; Frick, B. *J. Chem. Phys.* **2007**, *127* (14), 144910.
(17) Rittigstein, P.; Priestley, R. D.; Broadbelt, L. J.; Torkelson, J. M. *Nat. Mater.* **2007**, *6* (4), 278–282.
(18) Harton, S. E.; Kumar, S. K.; Yang, H.; Koga, T.; Hicks, K.; Lee, H.; Mijovic, Y.; Liu, M.; Vallery, R. S.; Gidley, D. W. *Macromolecules* **2010**, *43* (7), 3415–3421.
(19) Kropka, J. M.; Sakal, V. G.; Green, P. F. *Nano Lett.* **2008**, *8* (4), 1061–1065.
(20) Akcora, P.; Liu, H.; Kumar, S. K.; Moll, J.; Li, Y.; Benicewicz, B. C.; Schadler, L. S.; Acehan, D.; Panagiotopoulos, A. Z.; Pryamitsyn, V.; Ganesan, V.; Ilavsky, J.; Thiyagarajan, P.; Colby, R. H.; Douglas, J. F. *Nat. Mater.* **2009**, *8* (4), 354–359.
(21) Li, C.; Han, J.; Ryu, C. Y.; Benicewicz, B. C. *Macromolecules* **2006**, *39* (9), 3175–3183.
(22) Li, C. Z.; Benicewicz, B. C. *Macromolecules* **2005**, *38* (14), 5929–5936.
(23) http://www.ncnr.nist.gov/instruments/hfbs/.
(24) Beaucage, G.; Kammler, H. K.; Pratsinis, S. E. *J. Appl. Crystallogr.* **2004**, *37* (4), 523–535.
(25) Beaucage, G.; Schaefer, D. W. *J. Non-Cryst. Solids* **1994**, *172−174* (PART 2), 797−805.
(26) Roe, R.-J., *Methods of X-ray and Neutron Scattering in Polymer Science*: Oxford University Press: Oxford, U.K., 2000.
(27) Percus, J. K.; Yevick, G. J. *Phys. Rev.* **1958**, *110* (1), 1–13.
(28) Scheffold, F.; Mason, T. G. *J. Phys.: Condens. Matter* **2009**, *21* (33), 332102.
(29) Beaucage, G. *J. Appl. Crystallogr.* **1996**, *29* (2), 134–146.
(30) Wang, X.; Foltz, V. J.; Rackaitis, M.; Böhm, G. G. A. *Polymer* **2008**, *49* (26), 5683–5691.
(31) Akcora, P.; Kumar, S. K.; Moll, J.; Lewis, S.; Schadler, L. S.; Li, Y.; Benicewicz, B. C.; Sandy, A.; Narayanan, S.; Illavsky, J.; Thiyagarajan, P.; Colby, R. H.; Douglas, J. F. *Macromolecules* **2010**, *43* (2), 1003–1010.
(32) Merabia, S.; Sotta, P.; Long, D. R. *Macromolecules* **2008**, *41* (21), 8252–8266.
(33) Berriot, J.; Montes, H.; Lequeux, F.; Long, D.; Sotta, P. *Europhys. Lett.* **2003**, *64* (1), 50–56.
(34) Montes, H.; Lequeux, F.; Berriot, J. *Macromolecules* **2003**, *36* (21), 8107–8118.
(35) Jouault, N.; Vallat, P.; Dalmas, F.; Said, S.; Jestin, J.; Boue, F. *Macromolecules* **2009**, *42* (6), 2031–2040.
(36) Montes, H.; Chaussée, T.; Papon, A.; Lequeux, F.; Guy, L. *Eur. Phys. J. E31* (3), 263−268.
(37) Merabia, S.; Sotta, P.; Long, D. R. *J. Polym. Sci., Part B: Polym. Phys. 48* (13), 1495−1508.
(38) Sargsyan, A.; Tonoyan, A.; Davtyan, S.; Schick, C. *Eur. Polym. J.* **2007**, *43* (8), 3113–3127.
(39) Sternstein, S. S.; Ramorino, G.; Jiang, B.; Zhu, A. J. *Rubber Chem. Technol.* **2005**, *78* (2), 258–270.
(40) Sternstein, S. S.; Zhu, A. J. *Macromolecules* **2002**, *35* (19), 7262–7273.

Macromolecules
ADDITIONS AND CORRECTIONS

Segmental Dynamics in PMMA-Grafted Nanoparticle Composites
[*Macromolecules* **2010** , *43*, 8275]. Pinar Akcora,* Shane E. Harton, Sanat K. Kumar,* Victoria Garcia Sakai, Yu Li, Brian C. Benicewicz, and Linda S. Schadler

Page 8275. In the original submission of this article, one coauthor, Shane E. Harton, was inadvertently omitted.

Page 8277. The Figure 1 caption and Figure 1C image have been corrected. For the bare silica/PMMA nanocomposite, atactic PMMA (Scientific Polymer Products) was used at a filler loading of 20 mass %. However, the underlying conclusions drawn from the data are unchanged.

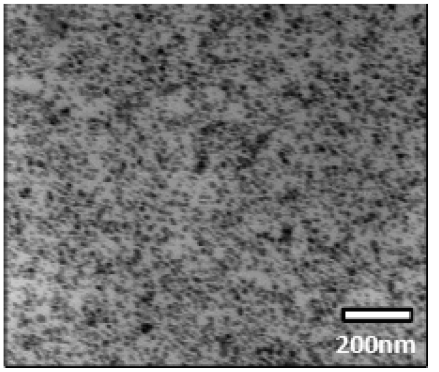

Figure 1. Transmission electron micrographs show the dispersion of PMMA grafted particles in immiscible composite A (part A) and in miscible composite B (part B). Images on the left were taken after 2 days of annealing and on the right after 30 days of annealing. Particle loadings are 15 mass % in parts A and B. Scale bars are 0.2 μm. For reference, we also show the dispersion of 20 mass % bare silica particles in atactic PMMA ($T_g \sim 110$ °C, $M_w \sim 75$ kg/mol) after annealing for 3 days at 160 °C. Clearly, good dispersion is seen in the last case.

DOI: 10.1021/ma102771k
Published on Web 12/31/2010